Journal of
Flood Risk Management

Sources of uncertainty in flood inundation maps

J.D. Bales and C.R. Wagner

US Geological Survey, Raleigh, NC, USA

Correspondence:
Jerad D. Bales, US Geological Survey, 3916 Sunset Ridge Road, Raleigh, NC 27607, USA
Email: jdbales@usgs.gov

This paper was presented at the 4th International Symposium on Flood Defence, Toronto, Canada (6–8 May 2008), and will be published in a special issue of *Journal of Flood Risk Management* entitled 'Integrated Flood (Risk) Management' edited by Professor Slobodan P. Simonovic, University of Western Ontario.

DOI:10.1111/j.1753-318X.2009.01029.x

Key words
Flood inundation mapping; floods; hydraulic modelling; uncertainty.

Abstract

Flood inundation maps typically have been used to depict inundated areas for floods having specific exceedance levels. The uncertainty associated with the inundation boundaries is seldom quantified, in part, because all of the sources of uncertainty are not recognized and because data available to quantify uncertainty seldom are available. Sources of uncertainty discussed in this paper include hydrologic data used for hydraulic model development and validation, topographic data, and the hydraulic model. The assumption of steady flow, which typically is made to produce inundation maps, has less of an effect on predicted inundation at lower flows than for higher flows because more time typically is required to inundate areas at high flows than at low flows. Difficulties with establishing reasonable cross sections that do not intersect and that represent water-surface slopes in tributaries contribute additional uncertainties in the hydraulic modelling. As a result, uncertainty in the flood inundation polygons simulated with a one-dimensional model increases with distance from the main channel.

Introduction

Maps depicting flood risk have been produced in the United States for almost 40 years by the Federal Emergency Management Agency (FEMA) through the National Flood Insurance Program (FEMA, 2009a). The purpose of these maps is to identify inundated areas associated with floods having identified exceedance levels, usually 0.2% and 1%, in an attempt to prevent or reduce flood damages. Similar efforts are underway as part of the European Union's (EU) Flood Directive, which calls for the development of flood hazard (likelihood of flooding) and flood risk (potential adverse consequences) maps for river basins and coastal zones in EU nations (European Commission, 2007). As in the United States, flood hazards and risks associated with specific exceedance levels are being produced.

In the United States, the National Weather Service (NWS) issues flood forecasts and warnings for about 2800 locations (NWS, 2009). Flood forecast products traditionally have included textual and graphical information on the expected flood peak in terms of river stage at the forecast point. In addition, the NWS qualitatively categorizes floods as major or moderate, based on river stage at the forecast point, but generally does not include information about exceedance levels in the forecast. These forecast products have been vital in mitigating impacts of floods across the nation, but the products are not easily interpretable by the public and some emergency responders. For example, river stage is generally reported to an arbitrary datum and readings can cause confusion (Pielke, 1999). Moreover, there is no readily available way to relate the forecast flood stage to the available flood risk maps produced for specific exceedance levels.

There is a growing recognition that more and better flood information is needed beyond that just described. Improved flood information products would (1) be available for more locations, (2) provide mapped information on inundated areas over a full range of river stages from bankfull to extremely low probability events, and (3) interface with a full suite of other flood-related products such as FEMA's Digital Flood Insurance Rate Maps (DFIRMs), the FEMA HAZUA-MH hazard loss application (FEMA, 2009b), and flood-forecast products produced by the NWS.

Massive inland flooding occurred in the aftermath of Hurricane Floyd (1999), which dropped more than 1 m of rainfall in parts of North Carolina (Bales *et al.*, 2000; Bales, 2003). In response, an initiative was launched to develop and demonstrate the technology for production of flood inundation maps for 18 locations in the Tar River basin, North Carolina (Figure 1), which suffered some of the worst flooding from the hurricane. Maps were produced over the full range of expected flows at each site, rather than for a few selected low-probability events (Bales *et al.*, 2007). The maps

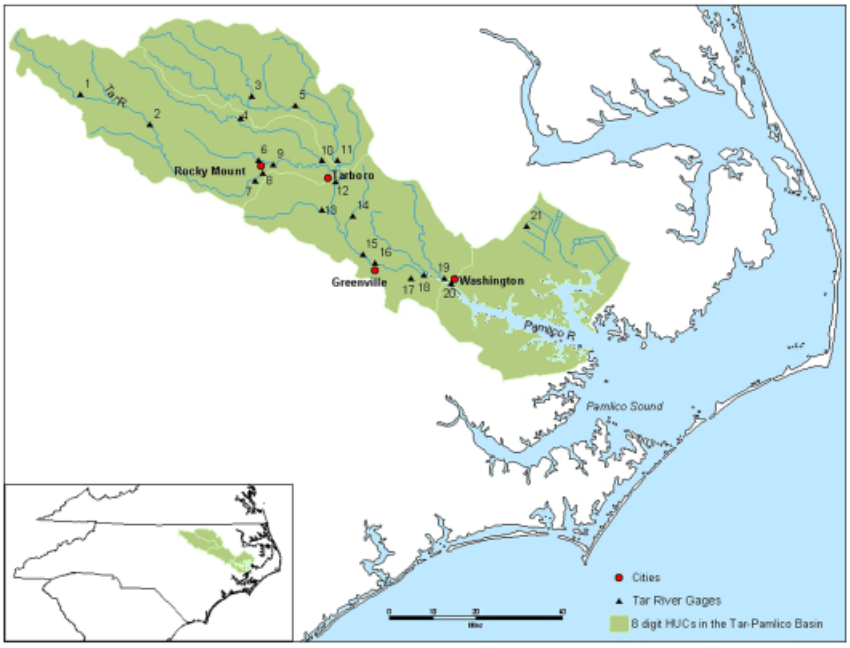

Figure 1 Location of Tar River basin in North Carolina, showing stream gauges and inundation map locations.

can be used in conjunction with real-time stream gauge measurements to depict current flooding (e.g. US Geological Survey, 2008), and to provide estimates of expected inundation in concert with NWS flood forecasts of expected peak water levels (e.g. NWS, 2008a). The NWS has since moved forward with inundation mapping at a number of locations across the United States using the methods developed in this study (NWS, 2008b).

Flood inundation maps represent the boundaries of expected inundated areas as a distinct line on a map, but there is a degree of uncertainty associated with the flood polygons – uncertainty that is typically unspecified. Nevertheless, because a map product is used to depict flood inundation, users often fail to recognize the inherent uncertainty associated with the maps.

The purpose of this paper is to describe sources of uncertainty associated with the creation of flood inundation maps produced from Light Detection and Ranging (LiDAR) topographic data and one-dimensional (1D) hydraulic models, which is the most common approach now used in the United States to produce inundation maps. Methods used to create flood inundation maps at selected stream gauge sites in the Tar River basin, North Carolina, are used to provide context for the discussion of uncertainty, but the focus of the paper is on sources of uncertainty rather than on Tar River hydraulic model performance.

The Tar River basin in North Carolina (Figure 1) has a drainage area of about 8300 km^2. The western one-third of the basin is in the Piedmont physiographic province, characterized by rolling terrain and shallow, poorly drained soils. The eastern part of the basin is in the Coastal Plain, characterized by little topographic relief, deep soils, and slow-moving streams. Annual average precipitation in the basin ranges from 116 cm in the west to 126 cm in the east (State Climate Office of North Carolina, 2006). The peak flow near the mouth of the basin following Hurricane Floyd was 2000 m^3/s, which was by far the greatest during more than 100 years of continuous annual flood records.

Sources of uncertainty in flood inundation maps

Although the flood inundation maps represent the boundaries of inundated areas with a distinct line on a map, there is some uncertainty associated with these maps, regardless of the way the maps were created. Quantitative analyses of uncertainty in inundation modelling have been reported, but these studies typically focus on only one source of uncertainty, such as the friction coefficient (Aronica *et al.*, 2002; Bates *et al.*, 2004), grid cell size (Werner, 2001), or flow characteristic (Purvis *et al.*, 2008). In addition, data required to apply rigorous methods of uncertainty analysis are seldom available (Beven, 2006), which was true for the Tar River mapping. Nevertheless, sources of uncertainty and the approximate magnitude of each of the sources for the Tar River basin inundation maps can be identified, which is the purpose of the following discussion.

Hydrologic data

Inundation maps were developed for Tar River stream reaches in the vicinity of 11 continuous recording streamflow gauges, at which stage–discharge relations were available over most of the complete range of observed flows, and eight continuous water-level gauges (Figure 1). The gauges were located on streams with drainage areas ranging from 290 to 2400 km^2. Water-level measurements are generally considered accurate to ± 0.3 cm. Streamflow data determined from stage–discharge ratings typically have an accuracy of between $\pm 5\%$ and 10%. Data from these gauges and from high-water marks, which might be considered accurate to ± 20 cm, from Hurricanes Floyd and Fran (Bales and Childress, 1996) were used to develop and test the hydraulic models.

Topographic data

Land-surface elevations are the dominant influence on the location of the simulated shoreline of the inundated area. Other studies have demonstrated that low-resolution 1D hydraulic modelling combined with high-resolution topographic data gives a good representation of the shoreline (Horritt and Bates, 2001). Thus, the quality of the resulting inundation map is highly dependent on the quality of the topographic data used to create the map. LiDAR was used to acquire land-surface elevation data in January–March 2001 (North Carolina Floodplain Mapping Program, 2003). Data were collected using a laser that pulsed at a rate of 4000–50 000 times/s. The raw data were subsequently processed to remove LiDAR returns from objects such as trees, buildings, and other structures.

Ground surveys were run by the North Carolina Geodetic Survey (2002) to at least 100 points in each county for which LiDAR data were collected. Survey points were distributed among five different land-cover classes, and the percentage of the survey points for each of the classes was approximately proportional to the percentage of each of the land-cover classes in the county. The root mean square elevation (RMSE) error (difference between control-point elevations and LiDAR elevations) for all of the counties in the Tar River basin was < 20 cm. There was little difference in the accuracy of the LiDAR data with topography. The RMSE error in the western, steeper part of the basin was 15.6 cm, compared with 16.1 cm in the middle of the basin and 16.4 cm in the downstream part of the basin, which has relatively little relief. At least for this basin, elevation error was more strongly related to land cover than to topography.

The absolute maximum difference between LiDAR-derived land-surface elevations and ground-survey elevations was about 40 cm for the Tar River basin counties, although the absolute maximum difference in most counties was < 30 cm. More than 50% of the LiDAR-derived elevations at the ground-control points were within 7 cm of the actual elevation for Tar River basin counties in which US Geological Survey stream gauges are located. In general, LiDAR-derived elevations tended to be higher than actual land-surface elevations. There was no real pattern in the relation between land cover and the maximum error, but the largest error tended to be associated with scrub or forested lands; the smallest error was associated with grass or developed land cover.

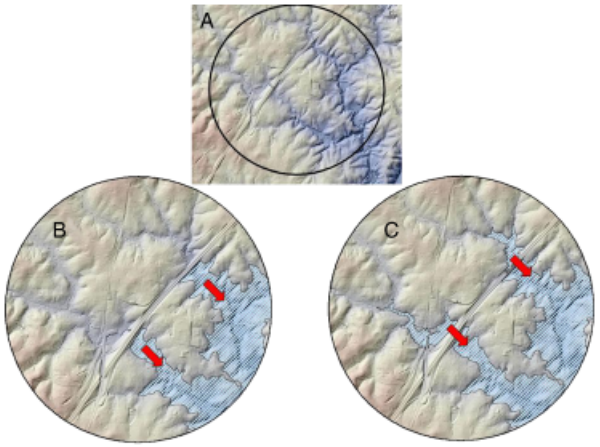

Figure 2 Example of hydro-conditioning, showing (a) hillshade digital elevation model and inundated area (b) before and (c) after hydro-conditioning. Red arrows indicate direction of streamflow. Note the absence of any inundation upstream from the highway before hydro-conditioning.

A simple calculation demonstrates the potential effects of topographic errors. Land surface slopes in the downstream (eastern) part of the Tar River basin are on the order of 0.1%. As a result, a change in elevation of 15 cm translates to a change in horizontal position of 150 m on a uniformly sloping plane, which the floodplain certainly is not. Nevertheless, small errors in elevation in this flat terrain can result in relatively large errors in the position of the shoreline.

Irregularly spaced LiDAR data were reprocessed into a digital elevation model (DEM) with regularly spaced, 1.5 m $\times$ 1.5 m cells. Because the LiDAR return signal is based on the reflection of the laser from a solid surface, the DEM maintains the elevation of bridges as the land-surface elevation at stream crossings, resulting in a discontinuous stream channel (Figure 2). The road as represented by the DEM becomes, in effect, a dam through which flow cannot pass. When calculating inundation areas from downstream to upstream locations, it is important that the DEM be hydro-conditioned so that the flow path is continuous along streambeds and low-lying areas, and this process can create some additional, poorly defined uncertainty (Merwade *et al.*, 2008). An automated script was developed for this study to connect flow paths (or streams) that were inappropriately disconnected by a bridge or road crossing (Figure 2)

in order to ensure consistent and thorough hydro-conditioning, resulting in the proper representation of inundated areas.

Following reprocessing of LiDAR data and hydro-conditioning of the DEM, all elevation surfaces in areas that would potentially be inundated were carefully reviewed. Two steps were taken to identify potential problems with DEMs. First, the maximum and minimum elevation was examined within each river reach for which inundation maps were to be developed. If values were unexpectedly high or low, the area was subsequently visually examined for problems. Second, after inundation polygons were developed, all inundated areas were examined for the presence of islands and to ensure that hydro-conditioning was complete. When islands were identified, orthophotographs were examined to determine if the feature creating the island on the DEM could be documented in the orthophotograph. Land-surface elevations that were found to be in error and affected the inundation mapping results were smoothed to surrounding elevations.

Hydraulic modelling

Development and calibration

Version 3.1.2 of the 1D, step-backwater (steady flow) model Hydraulic Engineering Center-River Analysis System (HEC-RAS) was used for hydraulic modelling (Hydrologic Engineering Center, 2006, 2002). Eleven individual hydraulic models were developed for the Tar River basin sites. Seven models were developed for reaches with a single gauge, and four models were developed for reaches in which there were multiple gauges near one another. Combined, the Tar River hydraulic models included 272 km of streams in the basin, including about 162 km on the Tar River mainstem and 59 bridges. Cross-section density in the models was about one cross section per 400 m of stream length.

Flood inundation models require four types of data: (1) topographic data for the hydraulic model computational grid and the inundation maps; (2) boundary conditions at the upstream and downstream ends of the model domain; (3) effective friction values (Manning's n) for each computational segment (1D model) or cell (2D model); and (4) model validation data (Bates, 2004). Inundation forecast models applied in near-real time also require a forecast inflow hydrograph. Uncertainties exist in each of these data types.

Bathymetric and topographic data used to develop the Tar River inundation models were derived from existing hydraulic models previously developed for DFIRM calculations, LiDAR data, field surveys, and interpolation of measured information. Bathymetric data were collected from bridges and manned boats utilizing graduated survey rods in shallow streams and acoustic instruments in deeper creeks and rivers. Overbank topography was developed from the 1.5 m × 1.5 m DEM.

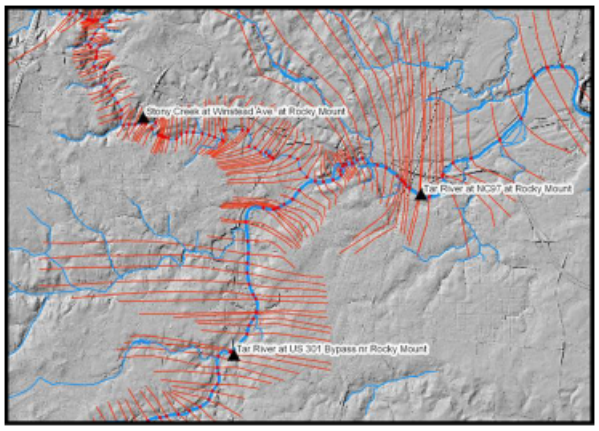

Figure 3 Example of cross sections in Tar River hydraulic model.

The floodplain in the Tar River models was represented by extended cross sections, rather than user-delineated storage areas. Overbank cross sections in 1D models generally should be approximately perpendicular to the stream at the point the cross section intersects the stream, and each cross section should intersect the main channel only once. In addition, two cross-section lines may not intersect each other. Many of the streams in the study area are quite sinuous, and so great care was required to develop overbank cross sections that met these requirements. Even so, there were cases, such as near the confluence of a tributary with the main channel, that it was not possible for the overbank cross section to be perpendicular to both the main channel and the tributary (e.g. Figure 3). As a result, the extrapolated inundation surface along tributaries may not be accurate.

Downstream boundary conditions for the Tar River models were established using the normal depth condition, with a friction slope estimated from the streambed slope through the reach. The normal depth was calculated by using the Manning equation. A measured or synthesized stage–discharge relation was used as the upstream boundary for each model.

The hydraulic models were calibrated to the most current stage–discharge relations (where available), to medium- to high-flow discharge measurements, and to high-water marks from recent regional floods. Calibration was achieved by adjusting Manning n values and the topography within reasonable limits, as well as adjusting boundary conditions for the cases in which boundaries were based on normal depth or synthetic stage–discharge ratings. Models were calibrated for water levels ranging from approximately bankfull at the gauge to the 0.2% exceedance level flow or to Hurricane Floyd peak stages, whichever was greater. The correlation coefficient between measured and simulated rating curves at nine of the 11 sites with measured rating

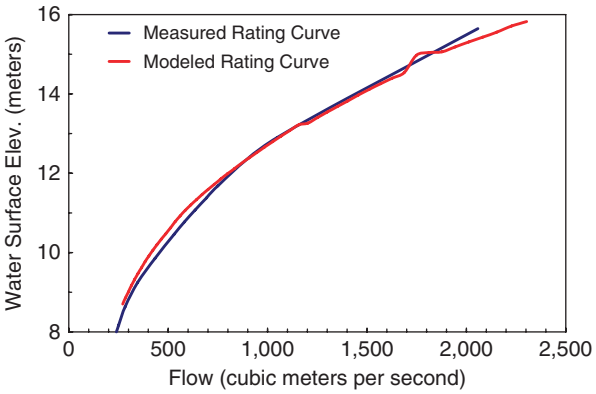

Figure 4 Measured and modelled ratings curves for Tarboro (Figure 1) hydraulic model.

curves was 0.99, and simulated rating curves matched measured curves over the full range of flows at the nine sites (e.g. Figure 4). At the two sites without measured rating curves, model performance was evaluated by comparing measured and simulated water levels; in some cases these water levels were from automated stage gauges, and in other cases the only measurements were high water marks. Differences between measured and simulated water levels for a specified flow at all sites (including those with and without measured rating curves) were no more than 0.44 m.

Friction values, or Manning's *n*, account for effects of variable cross sections, nonuniform slope, vegetation, and structures at the subgrid scale. Distributed data throughout the floodplain are seldom available as a basis for estimating friction values for the model domain. Studies also have shown that many different model parameter sets can perform equally well in 1D models (Pappenberger *et al.*, 2005), which represents uncertainty in the model, regardless of the goodness of fit between measured and simulated values. Moreover, the Manning formula was developed for uniform flow, which is not present during flood flows, and the equation is dimensionally nonhomogeneous. Hence, many of the uncertainties in 1D hydraulic models are lumped in the Manning *n* value.

Adequate calibration data are seldom available for inundation models, and this was true for the Tar River models. As previously noted, the Tar River models were calibrated by using measurements and simulations at a single point, or a few locations, which is the normal practice (Horritt and Bates, 2002). Because the models are used to simulate areal inundation, single-point calibration is not, however, the most desirable approach. In addition, stream gauge data can be in error by as much as 20% or more during extreme floods, and so improved methods for monitoring flood flows are needed (Bates *et al.*, 2006). Moreover, the extent of inundated area alone may not be sufficient to evaluate model performance, particularly for flat floodplains (Hesselink *et al.*, 2003). An ideal data set for flood inundation model calibration would include spatially detailed data on the inundation shoreline and, if the models are used to provide estimates of inundation depth, water depth data throughout the domain. Bates *et al.* (2006) collected four 1.2 m resolution synthetic aperture radar images from an aircraft during a flood on the River Severn in England. These images and the concurrent stream gauge data may be the most comprehensive flood inundation set available, and provide the type of time-varying point information on flood depth and spatial information on flood extent needed for effective model testing.

A set of steady-flow water-surface profiles was generated at 0.305 m increments for each of the modelled reaches. Based on the water-surface profile, a water-surface elevation was assigned to each cross section in the reach; the water surface was assumed to be level across the cross section, which is consistent with the 1D modelling approach. Water-surface elevations between cross sections were estimated using a spline interpolation. Inundated areas were identified by subtracting the water-surface elevation in each grid cell from the land-surface elevation in the cell. An automated procedure was developed to identify all inundated cells that were hydraulically connected to the cell at the downstream-most gauge in the model domain. This process resulted in a set of inundation map libraries for each modelled reach. Inundation polygons were merged with a variety of other geospatial data to provide information for flood mitigation and emergency response (e.g. Figure 5).

Effect of steady-flow assumption

Inundation maps developed using steady-flow modelling are based on the assumption that the flood flow has been constant for a period sufficiently long for all lands that could be flooded at that flow have, in fact, become inundated. This assumption clearly has less of an effect on inundation maps produced for lower flows than for higher flows because more time is typically required to inundate areas at higher flows. A flood at a given location for which water levels rise slowly to the peak, and then fall slowly, will most likely result in more inundation than a flood with the same peak flow, but which rises and falls quickly.

One of the Tar River basin models was used to demonstrate the effects of unsteady-flow simulations (Hydrologic Engineering Center, 1993) on estimates of flood inundation by simulating the Hurricane Floyd flood flows during September 1999. The relation between the measured water level and the simulated discharge at the site is shown in Figure 6. The blue arrows on the curve indicate rising or falling stage. There were, for example, four different water levels associated with the flow of 360 m^3/s, occurring on 9 September during a rising water level, 14 September during

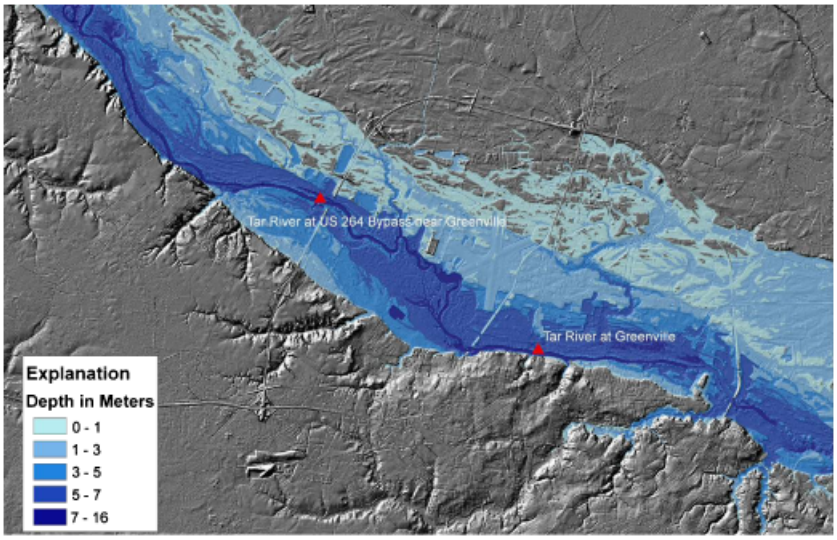

Figure 5 Estimated flood water depth for the water-surface elevation of 7.9 m above NAVD 88 at Greenville, North Carolina.

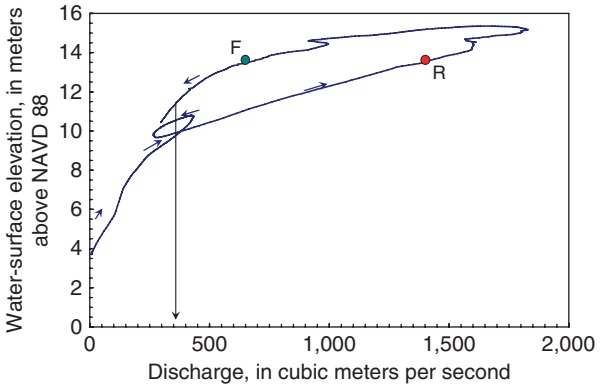

Figure 6 Measured water level – simulated discharge relation for Tar River at Tarboro during Hurricane Floyd flood of 5–30 September 1999; arrow depicts stages at a flow of 360 m^3/s, and 'R' and 'F' indicate rising and falling stage at an elevation of 13.7 m.

falling stage, 17 September during rising stage, and on 27 September during a falling stage. Water-surface elevations on these dates were 9.71, 10.55, 9.90, and 11.45 m above NAVD 88, respectively, for a range of about 1.7 m. Hence, an inundation map from the map libraries (0.035 m increment) for a flow of 360 m^3/s could have been selected from among seven different maps (9.7, 10.0, 10.3, and so on to 11.3 m above NAVD 88). According to the simulations, the inundated areas for the two occurrences of a water-surface elevation of 13.7 m (depicted as 'R' and 'F' in Figure 5) differed by more than 700 000 m^2, or more than 10% of the inundated area, with more area inundated during the falling water level, despite the fact that the flow was less than half the flow at the same water level on the rising side of the hydrograph.

The peak flow for a given exceedance level seldom occurs during steady-flow conditions, but FEMA flood insurance rate maps and inundation maps are typically created by assuming steady-flow conditions. Failure to attain steady-flow results in variable inundation extents for a single river flow (or stage) because a stable distribution of water in the floodplain is not attained. Additional research is needed on the relation between attainment of steady flow and the lateral distribution of water in the floodplain.

An alternative to the use of the steady-flow assumption and development of inundation map libraries, as was done for this project, is to estimate inundated areas in real time during, or immediately before, a flood so that the particular characteristics of the rainfall and flood hydrograph are well represented in the hydraulic modelling. Research applications have demonstrated that it is possible to produce reasonable inundation maps from medium-range weather forecasts (Pappenberger *et al.*, 2005) or from NWS estimates of rainfall derived from NEXRAD weather radar (Whiteaker *et al.*, 2006). The limitation of this approach is that the models must be run operationally in real time for each event and that results must be distributed quickly to emergency management officials and all other interested parties. Moreover, there will be some uncertainty in the forecast flows to the reach for which the inundation modelling is to be conducted (Bates, 2004). The infrastructure and funding for such a system is not in place for most locations in the United States, and so the steady-flow assumption and map-library approach currently offer some operational advantages. Further studies are needed to document any benefits of the real-time system over the map-library approach and to demonstrate the conditions for which each approach is more appropriate.

2D modelling

The 1D modelling approach used in this study resulted in good agreement between measured and simulated stage–-discharge ratings at sites where these ratings were available, and good agreement between measured and simulated stage and discharge observations at other sites. 1D models are relatively easy to construct, and simulations can be made quickly. 1D hydraulic models are based on the assumption that the hydraulic variables (water-surface elevation, water-surface slope, velocity, and cross-sectional flow area) are uniform across a cross section and that primary variation in these variables is from upstream to downstream. This assumption is reasonable for a prismatic channel in a relatively narrow floodplain.

The limitations of the 1D approach can be seen, however, in Figure 3. Water levels simulated using a 1D model are assumed to be constant across each cross section, but several cross sections intersect at least five or more streams other than the Tar River. According to the 1D assumption, water levels are the same at each point the cross section intersects a tributary stream as in the Tar River. It is possible to build branching 1D models to partially avoid the problems associated with the 1D assumption, but it is not possible to avoid the problems altogether, as cross sections from different branches could eventually intersect at high flows. The conclusion from this discussion, then, is that uncertainty in the 1D flood inundation polygons increases with distance from the main channel for which water-surface slopes were simulated, particularly in broad floodplains with numerous tributaries.

2D models have been used to simulate inundation in cases with highly variable floodplain topography. Studies have demonstrated that correct simulation of water storage in the floodplain near a channel is important for predicting flood-wave timing, and the increased lateral resolution of a 2D model allows proper simulation of this process (Horritt and Bates, 2001). Raster models, which use a 1D representation of channel flow linked to a simple model of flow between grids of cells on the floodplain, have been used to improve spatial resolution of flood inundation without significantly increasing computational requirements of the hydraulic model (e.g. Bates and De Roo, 2000). A coupled 1D–2D model was used to develop a library of flood inundation polygons for the Blue River, Missouri, where backwater from the Missouri River affects flows in the Blue River (Kelly and Rydlund, 2006). 2D models are particularly appropriate for simulating the passage of a flood hydrograph. Jones *et al.* (2002) used a fine-scale 2D model to simulate the movement of an NWS forecast flood hydrograph through the Snoqualmie River valley in Washington to produce forecast inundation along a 28 km reach of the river.

The raw LiDAR data that were processed to provide topographic information for the Tar River inundation modelling can also be processed to provide other information that could be useful for 2D modelling or for establishing a grid for a coupled 1D–2D model. For example, Cobby *et al.* (2001) used LiDAR data to not only delineate the flood plain topography for a 2D model, but also to estimate vegetation height, which would be used in flood inundation model to determine friction coefficients. Different algorithms were used in different vegetation types. In fact, a 2D model grid may be easier to establish with LiDAR data than an extended cross-section 1D model.

Conclusions

High-quality topographic data, along with the appropriate application of hydraulic modelling, are likely the most important factors required for accurate inundation maps. The assumption of steady flow, which typically is made for inundation map development, can have a major effect on simulated inundation, as the natural system responds differently to a dynamic flood than to an infinitely long steady flow. As a result, unsteady-flow models may be required in some cases, although these tools can be difficult to implement operationally.

Creators and users of flood inundation maps need to be mindful of uncertainties and sources of uncertainties associated with these maps, and that mapped flood inundation boundaries, although visually appealing, is likely not correct. Because of these uncertainties, flood boundaries might more reasonably be replaced with zones depicting probability of flooding (Brown and Damery, 2002; Werner, 2004; Smemoe *et al.*, 2007), and clear depiction of probability remains an area of research. However, some types of flood inundation maps are used as legal documents, for which uncertainty is not acceptable. Moreover, the public typically is untrained in interpreting risk and uncertainty, and generally wants concrete answers rather than ambiguities (Covello *et al.*, 2004). As a result, the institutional and social challenges associated with presenting uncertainties in flood boundaries may outweigh the technical issues.

References

Aronica G., Bates P.D. & Horritt M.S. Assessing the uncertainty in distributed model predictions using observed binary pattern information within GLUE. *Hydrol. Process.* 2002, **16**, 2001–2016.

Bales J.D. Effects of Hurricane Floyd inland flooding, September–October 1999, on Tributaries to Pamlico Sound, North Carolina. *Estuaries* 2003, **26**, (5), 1319–1328.

Bales J.D. & Childress C.J.O. Aftermath of Hurricane Fran in North Carolina – preliminary data on flooding and water

quality. US Geological Survey Open-File Report 96-499, 6pp., 1996.

Bales J.D., Oblinger C.J. & Sallenger A.H. Jr. Two months of flooding in eastern North Carolina, September–October 1999 – hydrologic, water quality, and geologic effects of hurricanes Dennis, Floyd, and Irene. US Geological Survey Water-Resources Investigations Report 00-4093, 47pp., 2000.

Bales J.D., Wagner C.R., Tighe K.C. & Terziotti S. LiDAR-derived flood-inundation maps for real-time flood-mapping applications, Tar River basin, North Carolina. US Geological Survey Scientific Investigations Report 2007-5032, 42pp., 2007.

Bates P.D. Remote sensing and flood inundation modelling. *Hydrol. Process.* 2004, **18**, 2593–2597.

Bates P.D. & De Roo A.P.J. (2000). A simple raster based model for flood inundation simulation. *J. Hydrol.*, **236**, 54–77.

Bates P.D., Horritt M.S., Aronica G. & Beven K. Bayesian updating of flood inundation likelihoods conditioned on flood extent data. *Hydrol. Process.* 2004, **18**, 3347–3370.

Bates P.D., Wilson M.D., Horritt M.S., Mason D.C., Holden N. & Currie A. Reach-scale floodplain inundation dynamics observed using airborne synthetic aperture radar imagery: data analysis and modelling. *J. Hydrol.* 2006, **328**, 306–318.

Beven K. On undermining the science? *Hydrol. Process.* 2006, **20**, 3141–3146.

Brown J.D. & Damery S.L. Managing flood risk in the UK; toward an integration of social and technical perspectives. *Trans. Br. Inst. Geogr.* 2002, **27**, 412–426.

Cobby D.M., Mason D.C. & Davenport I.J. Image processing of airborne scanning laser altimetry data for improved river flood modelling. *J. Photogramm. Remote Sensing* 2001, **56**, 121–138.

Covello V.T., McCallum D.B. & Pavlova M.T., eds. *Effective risk communication: the role and responsibility of government and nongovernment organizations*. New York: Plenum Publishing Corporation, 2004, 388pp.

European Commission. Directive 2007/60/EC of the European Parliament and of the Council of 23 October 2007 on the assessment and management of flood risks. Available at http://eur-lex.europa.eu/LexUriServ/LexUriServ.do?uri=CELEX:32007L0060:EN:NOT [accessed 19 March 2009], 2007.

Federal Emergency Management Agency (FEMA). National Flood Insurance Program. Available at http://www.fema.gov/plan/prevent/fhm/index.shtm [accessed 19 March 2009], 2009a.

Federal Emergency Management Agency (FEMA). Using HAZUS-MH. Available at http://www.fema.gov/plan/prevent/hazus/hz_app.shtm [accessed 19 March 2009], 2009b.

Hesselink A.W., Stelling G.S., Kwadijk J.C.J. & Middelkoop H. Inundation of a Dutch River Polder, sensitivity analysis of a physically based inundation model using historic data. *Water Resour. Res.* 2003, **39**, (9), 1234, doi: 10.1029/2002WR001334.

Horritt M.S. & Bates P.D. Effects of spatial resolution on a raster based model of flood flow. *J. Hydrol.* 2001, **253**, 239–249.

Horritt M.S. & Bates P.D. Evaluation of 1D and 2D numerical models for predicting river flood inundation. *J. Hydrol.* 2002, **268**, 87–99.

Hydrologic Engineering Center. *UNET, one-dimensional unsteady flow through a full network of open channels, user's manual*. Davis, CA: US Army Corps of Engineers, 1993.

Hydrologic Engineering Center. *HEC-RAS river analysis system user's manual, version 3.1, computer program documentation report 68*. Davis, CA: US Army Corps of Engineers, 2002. Available at http://www.hec.usace.army.mil/software/hec-ras/hecras-document.html [accessed 30 August 2006].

Hydrologic Engineering Center. HEC-RAS 3.1.3 release notes. Available at http://www.hec.usace.army.mil/software/hec-ras/documents/HEC-RAS3.1.3_Release%20Notes.pdf [accessed 30 August 2006], 2006.

Jones J.L., Fulford J.M. & Voss F.D. Near-real-time simulation and internet-based delivery of forecast-flood inundation maps using two-dimensional hydraulic modeling – a pilot study for the Snoqualmie River, Washington. US Geological Survey Water-Resources Investigations Report 2002-4251, 40pp., 2002.

Kelly B.P. & Rydlund P.H. Estimated flood-inundation mapping for the lower Blue River in Kansas City Missouri, 2003–2005. US Geological Survey Scientific Investigations Report 2006-5089, 2006.

Merwade V., Olivera F., Arabi M. & Edleman S. Uncertainty in flood inundation mapping: current issues and future directions. *J. Hydrol. Eng.* 2008, **13**, (7), 608–620.

National Weather Service (NWS). Advanced Hydrologic Prediction Service, Tar River at Tarboro, CN (TARN7). Available at http://newweb.erh.noaa.gov/ahps2/inundation/inundation.php?wfo=rah&gage=tarn7&view=1,1,1,1,1,1&toggles=10,7,8,2,9,15,6 [accessed 30 November 2008], 2008a.

National Weather Service (NWS). Inundation mapping locations. Available at http://www.weather.gov/ahps/inundation.php [accessed 30 November 2008], 2008b.

National Weather Service (NWS). River forecasts. Available at http://www.weather.gov/ahps/forecasts.php [accessed 19 March 2009], 2009.

North Carolina Floodplain Mapping Program. LiDAR and digital elevation data fact sheet. Available at http://www.ncfloodmaps.com/pubdocs/lidar_final_jan03.pdf [accessed 23 August 2006], 2003.

North Carolina Geodetic Survey. LiDAR quality control status page. Available at http://www.ncgs.state.nc.us/flood/qc_reports/qc_status.htm [accessed 23 August 2006], 2002.

Pappenberger F., Beven K.J., Horritt M. & Blazkova S. Uncertainty in the calibration of effective roughness parameters in HEC-RAS using inundation and downstream water level observations. *J. Hydrol.* 2005, **302**, 46–69.

Pielke R.A. Jr. Who decides? Forecasts and responsibilities in 1997 Red River flood. *Appl. Behav. Sci. Rev.* 1999, **7**, (2), 83–101.

Purvis M., Bates P.D. & Hayes C.M. A probabilistic methodology to estimate future coastal flood risk due to sea level rise. *Coastal Eng.* 2008, **55**, 1062–1073.

Smemoe C.M., Nelson E.J., Zundel A.K. & Woodruff-Miller A. Demonstrating floodplain uncertainty using flood probability maps. *J. Am. Water Resour. Assoc.* 2007, **43**, (2), 359–371.

State Climate Office of North Carolina. NC Climate Retrieval and Observations Network of the Southeast Database. Available at http://www.nc-climate.ncsu.edu/cronos/ [accessed 23 August 2006], 2006.

US Geological Survey. Tar-River basin inundation mapping. Available at http://nc.water.usgs.gov/finmap/ [accessed 10 March 2008], 2008.

Werner M.G.F. Impact of grid size in GIS based flood extent mapping using a 1D flow model. *Phys. Chem. Earth Part B – Hydrol. Oceans Atmos.* 2001, **26**, (7–8), 517–522.

Werner M.J.F. A comparison of flood extent modelling approaches through constraining uncertainties on gauge data. *Hydrol. Earth Syst. Sci.* 2004, **8**, (6), 1141–1152.

Whiteaker T.L., Robayo O., Maidment D.R. & Obenour D. From a NEXRAD rainfall map to a flood inundation map. *J. Hydrol. Eng.* 2006, **11**, (1), 37–45.